

Optical properties of glass with trailing indent cracks during chemical etching

Huapan Xiao^{1,#}, Chi Fai Cheung^{1,#}, Shenxin Yin², Chunjin Wang¹

¹ State Key Laboratory of Ultra-precision Machining Technology, The Hong Kong Polytechnic University, Hung Hom, Kowloon, Hong Kong

² College of Aerospace Engineering, Chongqing University, Chongqing 400044, China

Corresponding Author / Email: hp0698.xiao@polyu.edu.hk; benny.cheung@polyu.edu.hk

KEYWORDS: Ultra-precision machining, Chemical etching, Optical properties, Glass, Trailing indenter cracks

In this paper, chemical etching experiments were carried out on two K9 glasses with trailing indent cracks (TICs). The surface morphology of etched TICs and the optical properties of the glass with etched TICs are analyzed firstly. The results show that the transmissivity of the glass with TICs initially decreases and then increases with the increase of etching time. Conversely, the reflectivity initially increases and then decreases. This can be attributed to morphological evolution of TICs during chemical etching. Then, based on the fact that TICs are a series of spaced cracks, a simulation model is developed for determining the optical properties of the glass with etched TICs. The model is validated experimentally. It is found that the model is effective when the light wavelength is large and the TICs are uniformly distributed. This research contributes to improving the optical properties of polished optical glasses by chemical etching.

1. Introduction

Chemical etching has emerged as a promising and effective precision machining method for processing optical glasses in various applications. For example, Zheng et al. [1] found that the damage resistance of fused silica could be significantly enhanced by slight HF etching. In addition, the etched surface exhibited a higher hardness compared to the original material. Maeng et al. [2] discovered that the light transmissivity of soda lime glass decreased seriously while the strength increased after HF etching. The main reason why chemical etching is widely applied is that it can reveal hidden micro-cracks, decrease the length of micro-cracks, and blunt the tips of micro-cracks in optical glasses [3, 4]. Correlating the surface morphology of micro-cracks with the service performance of optical glass is significant. Trailing indent cracks (TICs) are the most common crack characteristics found in polished optical glass [5]. However, the morphological evolution of TICs and their influence on the optical properties of optical glass have not been well understood during chemical etching. To address this problem, compared with the surface morphology of etched TICs, the optical properties of the glass with etched TICs were analyzed experimentally. Meanwhile, a simulation model is developed for determining the optical properties of the glass with etched TICs. The experimental and simulated optical properties were compared to validate the model. The research contributes to the ultra-precision machining of optical glass by chemical etching.

2. Experimental Analysis of Optical Properties

2.1 Experimental Procedure

Three K9 glasses ($\Phi 25.4 \times 4$ mm) were polished using the same process parameters. The buffered oxide etch (BOE) solution were prepared by combining 18.75% (wt) HF solution with 40% (wt) NH_4F . As shown in Fig. 1, glass 1 and glass 2 were etched with the BOE solution at $\text{HF}:\text{NH}_4\text{F} = 1:3$ and $1:6$, respectively, and glass 3 was not subjected to any etching. The etching temperature was 40°C . The surface morphologies of glass 1 and glass 2 were observed by laser scanning confocal microscopy (OLS4000, Olympus Corporation, Japan). The optical properties of glass 1, glass 2, and glass 3 were measured by UV-visible spectrophotometry (UV-3600, Shimadzu Corporation). The surface morphologies and optical properties of glass 1 and glass 2 etched for each 10 min were measured. During the measurement, the black adhesive tape was used to locate the TICs concerned. Before each measurement, the glass was cleaned with alcohol, acetone, and plasma water for 5 minutes, respectively, using an ultrasonic cleaning machine.



Fig. 1 Three K9 glasses prepared.

2.2 Experimental Result and Discussion

When abrasive particles slide or roll during polishing, the morphology of the fractures would be a TIC, which appears as a series of arcs. Since the motion and size of abrasive particles are random, the positions and sizes of TICs are usually different. The surface morphologies of etched TICs from glass 1 and glass 2 are shown in Fig. 2(a) and Fig. 3(a). The TICs consist of a series of spaced cracks. The crack width gradually increases and eventually the adjacent cracks coalesce together with the increase of etching time. The etched TICs marked with an ellipse are selected, as shown in Fig. 2(a) and Fig. 3(a), and their surface profiles are extracted, as shown in Fig. 2(b) and Fig. 3(b). In Fig. 3(b), the surface profile etched for 10 min is significantly different from that for 20 min, which could be attributed to the presence of tiny cracks within the TICs. These tiny cracks are not fully visible until they have been etched for 20 min. The surface profile with etched TICs becomes initially rough and then smooth with the increase of etching time. The surface roughness is due to the expansion of cracks, while the smoothness is caused by the coalescence of adjacent cracks. This demonstrates that the surface profile of TICs can be smoothed by chemical etching. In this paper, the TICs etched for 10 min and 60 min from glass 1 are defined as cracks (I) and cracks (III), respectively. The TICs etched for 20 min and 60 min from glass 2 are defined as cracks (II) and cracks (IV), respectively. Cracks (I) or (III) have 23 small cracks, while cracks (II) or (IV) have 16 small cracks.

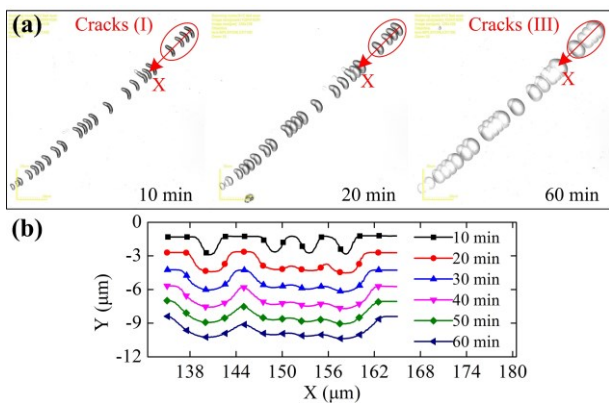


Fig. 2 (a) Surface morphologies and (b) surface profiles of etched TICs from glass 1.

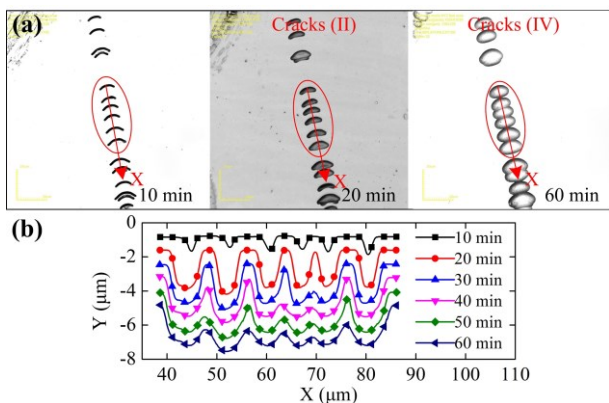


Fig. 3 (a) Surface morphologies and (b) surface profiles of etched TICs from glass 2.

Six regions are defined, region 0 from glass 3, region 1 with cracks (I), region 2 without any cracks from etched glass 1, region 3 with cracks (II), region 4 without any cracks from etched glass 2, region 5 with cracks (III), and region 6 with cracks (IV). The measured transmissivity (T) and reflectivity (R) curves of region 0 to region 5 are showed in Fig. 4(a) and Fig. 4(b). It can be observed that the curves fluctuate when the wavelength is around 700 nm. This is because the spectrophotometry needs to replace the light source when irradiating at this wavelength, which leads to instability in the measured results. It can be also observed that the transmissivity of region 3 is lower than that of region 1, while the reflectivity is higher; and the transmissivity of region 1 is lower than that of region 0, while the reflectivity is higher. The transmissivity and reflectivity of regions 2, 4, 5, and 6 are almost the same as that of region 0.

The further analysis is presented as follows. Compared with glass 3, the transmissivity of the glass with TICs etched for 10~20 min is smaller, while the reflectivity is larger. Nevertheless, the glass with TICs etched for 60 min nearly has the same transmissivity and reflectivity as glass 3. This may be because the TICs are opened and the transmissivity decreases at the initial stage of chemical etching, while the TICs gradually coalesce together with the increase of etching time. In other words, as the etching time increases, the transmissivity of the glass with TICs initially decreases and then increases, while the reflectivity initially increases and then decreases. This suggests that chemical etching can alter the optical properties of optical glass with micro-cracks.

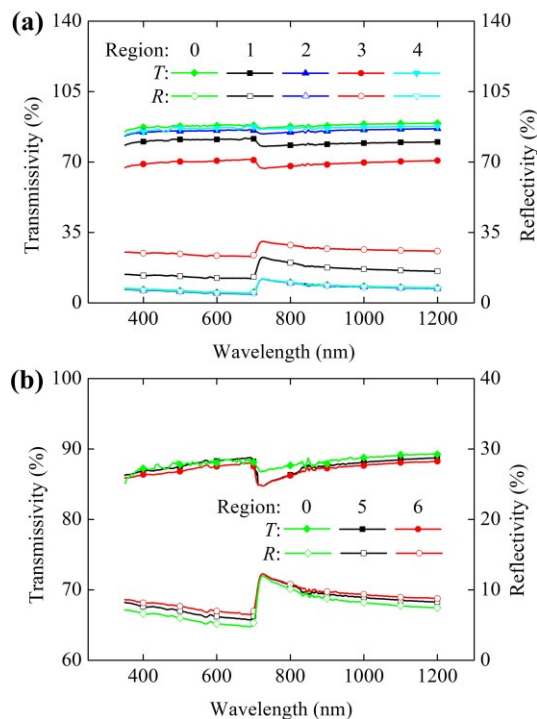


Fig. 4 (a) The transmissivity (T) and reflectivity (R) curves of region 0, region 1 to region 4; (b) the transmissivity (T) and reflectivity (R) curves of region 0, region 5, and region 6.

3. Numerical Simulation of Optical Properties

3.1 Simulation Model

A simulation model is developed for determining the optical properties of the glass with etched TICs. The thickness of glass is much greater than the wavelength of light. As shown in both Fig. 5(a) and Fig. 5(b), a control domain is defined. The top side of the control domain is where the incident light enters. The blank and gray areas represent air and glass, respectively, and the shadow area corresponds to the perfectly matched layer (PML). A parallel light is vertically incident into the air in Fig. 5(a), while it is vertically incident into the glass with an etched TIC in Fig. 5(b). The PML can absorb electromagnetic waves without any reflection, and its absorption performance remains stable even when the incident angle is very large. A closed curve is defined to collect the transmission power. The control equations are Maxwell's equations:

$$\begin{cases} \partial \mathbf{B} / \partial t = -\nabla \times \mathbf{E} & \nabla \times \mathbf{D} = \rho \\ \partial \mathbf{D} / \partial t = \nabla \times \mathbf{H} - \mathbf{J} & \nabla \times \mathbf{B} = 0 \end{cases} \quad (1)$$

where \mathbf{B} is the magnetic induction intensity; \mathbf{E} is the electric field intensity; \mathbf{D} is the dielectric flux density; ρ is the charge density; \mathbf{H} is the magnetic field intensity; and \mathbf{J} is the electric current density.

The constitutive equations of materials can be expressed as:

$$\mathbf{D} = \varepsilon_0 \mathbf{E} \quad \mathbf{B} = \mu_0 \mathbf{H} \quad \mathbf{J} = \sigma \mathbf{E} \quad (2)$$

where ε_0 is the dielectric constant of vacuum; μ_0 is the magnetic permeability of vacuum; and σ is the electric conductivity.

The incident light is defined as a transverse magnetic (TM) wave. The power of incident light is set as P_0 , and the transmission power is set as P_1 . The transmissivity T_1 and reflectivity R_1 of the glass with an etched TIC can be respectively expressed as:

$$\begin{cases} T_1 = P_1 / P_0 \\ R_1 = 1 - T_1 - A_1 \end{cases} \quad (3)$$

where A_1 is the absorptivity.

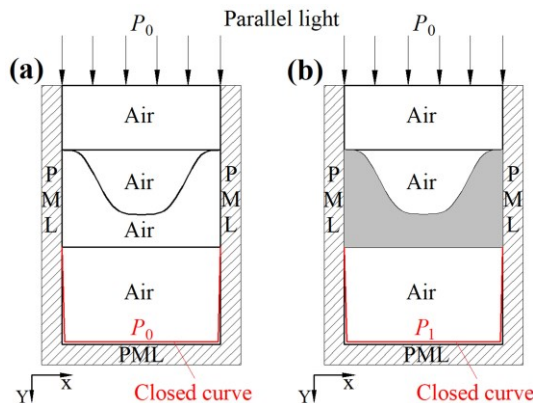


Fig. 5 A control domain for simulating the optical properties when (a) a parallel light is vertically incident into the air and (b) it is vertically incident into the glass with an etched TIC.

3.2 Simulation Result and Discussion

The size of an etched TIC for the simulation is obtained by averaging all small cracks from cracks (I) and cracks (II). The control equations are solved by software *COMSOL*. Fig. 6(a) shows the simulated electric field intensity E_x in the control domain with a smooth glass, and Fig. 6(b) shows the simulated electric field intensity E_x in the control domain with the glass containing an etched TIC from cracks (I). Since the incident light is a TM wave, the electric field intensity only has an x component. The light wavelength becomes short and propagates dispersedly after it passes through an etched TIC. The incident and reflected light overlap each other in the incident region, but only transmission light in the transmissive region. As a result, the distribution of electric field intensity in the incident region is denser than that in the transmissive region.

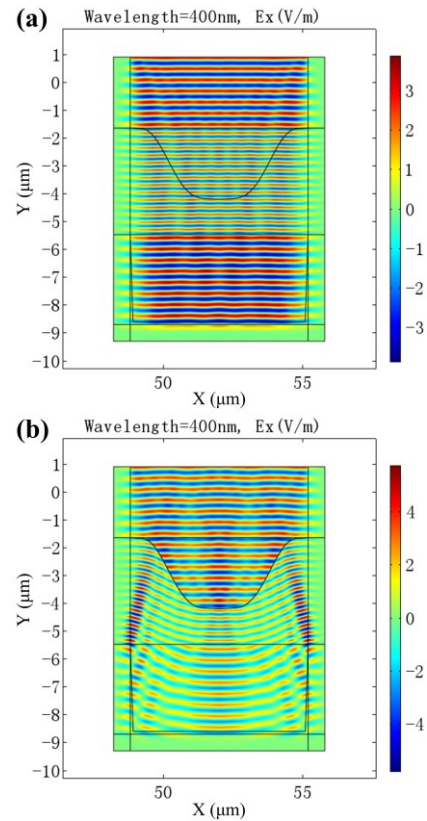


Fig. 6 (a) The simulated electric field intensity E_x in a smooth glass; (b) the simulated electric field intensity E_x in the glass with an etched TIC from cracks (I).

The simulation model considers the morphology while neglects the thickness. The experimental results consider the morphology and thickness of glass. As a result, the experimental results should be modified for the comparison with the simulated results. In this paper, the absorptivity A_{ay} is added to the experimental results by:

$$\begin{cases} T_m = T + TA_{ay} / (T + R) \\ R_m = R + RA_{ay} / (T + R) \\ A_{ay} = 1 - T_{avg} - R_{avg} \end{cases} \quad (4)$$

where T_m and R_m are the modified experimental values of

transmissivity and reflectivity, respectively; T_{avg} and R_{avg} are obtained by averaging the experimental values of transmissivity T and reflectivity R , as shown in Fig. 4(a).

Fig. 7(a) and Fig. 7(b) show the experimental and simulated curves of transmissivity and reflectivity of the glass with an etched TIC from cracks (I) and cracks (II). The curves fluctuate with the wavelength, and the simulated results (T_1 , R_1) coincide well with the experimental ones (T , R , T_m , and R_m) at a larger wavelength. The simulated curves from cracks (II) show better agreement with the experimental ones compared to those from cracks (I). This is likely due to the more uniform distribution of cracks (II). The average simulated values of transmissivity and reflectivity of the glass with an etched TIC from cracks (I) are 80.4% and 19.6%, respectively, while the values from cracks (II) are 70.1% and 25.7%, respectively. The modified experimental values of transmissivity and reflectivity from cracks (I) are 83.7% and 16.3%, respectively. For cracks (II), the corresponding values are 73.0% and 27.0%, respectively. Comparing the simulated results with the experimental ones, the error values of transmissivity and reflectivity from cracks (I) are 3.9% and 20.2%, respectively, and those values from cracks (II) are 4.0% and 4.8%, respectively. If the values of transmissivity and reflectivity at the wavelength of greater than 700 nm are taken the average for the comparison, the error values of transmissivity and reflectivity from cracks (I) are 1.3% and 0.6% respectively, while those values from cracks (II) are 0.4% and 2.1%, respectively. On the whole, to some extent, the simulation model can be used to determine the optical properties of the glass with TICs. This is particularly applicable when the wavelength is large and the TICs are uniformly distributed.

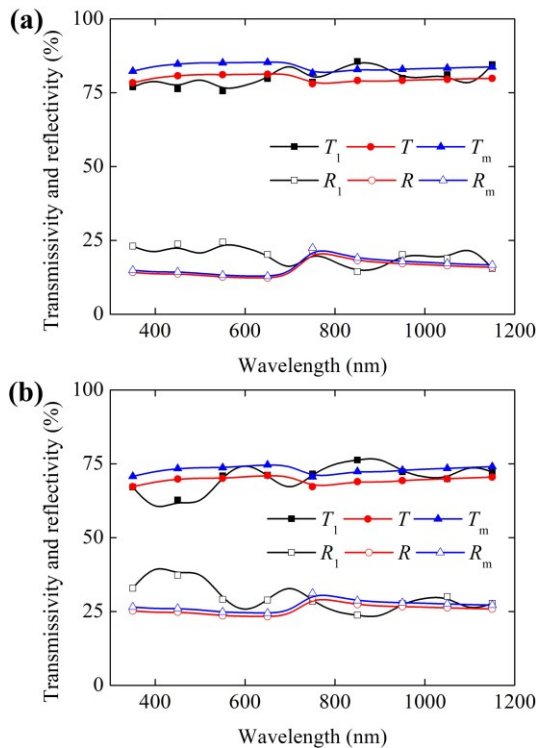


Fig. 7 Experimental and simulated curves of transmissivity (T_1 , T , T_m) and reflectivity (R_1 , R , R_m) of the glass with an etched TIC from (a) cracks (I) and (b) cracks (II).

4. Conclusions

In this paper, experimental analysis and numerical simulations are carried out for investigating the optical properties of the glass with TICs during chemical etching. The conclusions are given as follows:

- (1) When abrasive particles slide or roll during polishing, the morphology of the fractures appears as a series of arcs. This results in the TICs consisting of a series of spaced cracks.
- (2) With an increasing etching time, the transmissivity of the glass with TICs initially decreases and then increases, while the reflectivity initially increases and then decreases. This can be attributed to that as etching time increases, the crack width gradually increases and the adjacent cracks coalesce together.
- (3) The simulation model can be used to determine the optical properties of the glass with etched TICs, especially when the light wavelength is large and the TICs are uniformly distributed.

ACKNOWLEDGEMENT

The authors would like to express thanks to the National Key R&D Program of China (No. 2023YFE0203800), National Natural Science Foundation of China (52305509, 12104074), Innovation and Technology Commission (ITC) of the Government of the Hong Kong Special Administrative Region, China (MHP/151/22).

REFERENCES

1. Zheng, Z., Zu, X., Jiang, X., Xiang, X., Huang, J., Zhou, X., Li, C., Zheng, W., and Li, L., "Effect of HF etching on the surface quality and laser-induced damage of fused silica," *Opt. Laser Technol.*, Vol. 44, No. 4, pp. 1039-1042, 2012.
2. Maeng, J.-H., Kim, D.-H., Park, S.-M., and Kim, H.-J., "The effect of chemical treatment on the strength and transmittance of soda-lime cover glass for mobile," *Int. J. Precis. Eng. Manuf.*, Vol. 15, No. 9, pp. 1779-1783, 2014.
3. Wong, L., Suratwala, T., Feit, M. D., Miller, P. E., and Steele, R., "The effect of HF/NH₄F etching on the morphology of surface fractures on fused silica," *J. Non-Cryst. Solids*, Vol. 355, No. 13, pp. 797-810, 2009.
4. Ma, B., Lu, M., Zhan, G., Wang, K., Cheng, X., and Wang, Z., "Effect of etching morphology of artificial defect on laser-induced damage properties under 355 nm laser irradiation," *Appl. Opt.*, Vol. 54, No. 11, pp. 3365-3371, 2015.
5. Zhang, C., Xu, M., and Wang, C., "Light intensification effect of trailing indent crack in fused silica subsurface," *Sci. China-Phys. Mech. Astron.*, Vol. 58, No. 3, pp. 034201, 2014.